Tilted Gaussian beam propagation in inhomogeneous media

Yakir Hadad and Timor Melamed*

Department of Electrical and Computer Engineering, Ben-Gurion University of the Negev, Beer Sheva 84105, Israel
**Corresponding author: timormel@ee.bgu.ac.il*

Received April 26, 2010; revised June 11, 2010; accepted June 16, 2010;
posted June 24, 2010 (Doc. ID 127576); published July 22, 2010

The present work is concerned with applying a ray-centered non-orthogonal coordinate system which is *a priori* matched to linearly-phased localized aperture field distributions. The resulting beam-waveobjects serve as the building blocks for beam-type spectral expansions of aperture fields in 2D inhomogeneous media that are characterized by a generic wave-velocity profile. By applying a rigorous paraxial-asymptotic analysis, a novel parabolic wave equation is obtained and termed "Non-orthogonal domain parabolic equation"—NoDope. Tilted Gaussian beams, which are exact solutions to this equation, match Gaussian aperture distributions over a plane that is tilted with respect to the beam-axes initial directions. A numerical example, which demonstrates the enhanced accuracy of the tilted Gaussian beams over the conventional ones, is presented as well. © 2010 Optical Society of America

OCIS codes: 070.2580, 350.5500, 080.2720.

1. INTRODUCTION

Gaussian beams (GBs) have been a subject of intense continuous research mainly due to their joint spectral-spatial localization, which is significantly advantageous for propagation and scattering and results in simplified analytic expressions for the beam fields. Locality considerations have been utilized for solving beam-type waveobjects propagation in generic medium profiles such as inhomogeneous [1–3], anisotropic [4–10], and for time-dependent pulsed beams, in dispersive media [11–15]. The need for these solutions arises from beam-type expansions such as the frame-based field expansions [16–18]. These expansion schemes utilize the key feature of the beam's continuous spectrum [19–21] and discretize the spectral representation with no loss of accuracy.

Exact beam-type expansions require beam solutions that match localized initial planar distributions. Such solutions in inhomogeneous media can be obtained by applying the parabolic wave equation (PWE), which models propagation of linear waves that are predominant in one direction [22–27]. Important solutions of the PWE include its different beam-type waveobjects [28–30]. PWE methods can also be utilized for solving beam-type waveobjects propagation in inhomogeneous media [1–3].

In these solutions as well as in other different propagation scenarios, the boundary plane over which the initial field distribution is given is generally *not perpendicular* to the paraxial direction of propagation (the beam-axis). Therefore, in order to use conventional (orthogonal coordinates) GBs, apart from asymptotic approximations, an additional approximation is carried out to project the initial field complex curvature matrix on a plane *normal* to the beam-axis direction. This additional approximation reduces the accuracy of the resulting beam solutions especially for large angle departures and, moreover, it becomes *inconsistent with respect to asymptotic orders*.

The need for the additional approximation can be avoided by applying a *non-orthogonal* coordinate system that is *a priori* matched to the lineally phased aperture distribution. This system has been introduced in [31] and was applied for obtaining beam-type waveobjects in a 3D *homogeneous* medium. These waveobjects were termed "tilted GBs." Application of the scalar tilted GBs to electromagnetic beam-type expansions has been explored as well. Different types of tilted GBs were parameterized in [32]. The present investigation extends these results to include propagation in 2D *inhomogeneous* media that is identified by a generic wave-velocity profile. Thus, a novel form of PWE in non-orthogonal coordinates is obtained such that its beam-type solutions are matched to localized aperture distributions over tilted planes (see Fig. 1).

2. STATEMENT OF THE PROBLEM

Beam-type expansion schemes can be obtained by projecting the planar $z=0$ aperture field distribution on localized linearly-phased Gaussian windows. The field in $z>0$ half-space is described by a superposition of tilted beams that emanate from a discrete set of points over the aperture in a discrete set of directions. Each beam propagator is identified by a spectral wavenumber $\bar{k}$ that contributes to the aperture distribution a linear phase term of $i\bar{k}x$ [19,21]. This spectral wavenumber is related to the beam-axis spectral (departure) angle ϑ via $\cos\vartheta=V_0\bar{k}/\omega$, where V_0 is the wave velocity at the departure point (see Fig. 1). Thus the ability to apply beam-type expansions in inhomogeneous media depends on finding accurate beam solutions that match linearly-phased Gaussian aperture distributions.

We are concerned with asymptotically evaluating the 2D time-harmonic beam-field $u(x,z)$ in the $z>0$ half-

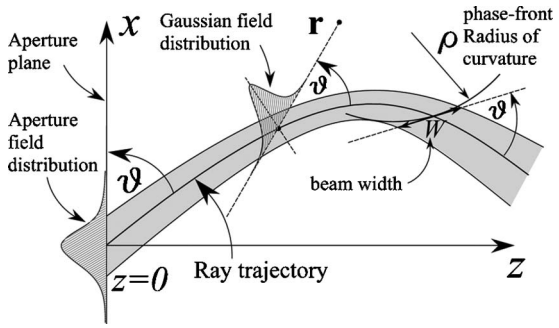

Fig. 1. Tilted Gaussian beam waveobject is propagating along a ray trajectory (beam-axis) in an inhomogeneous medium that is characterized by a generic wave-velocity profile $V(x,z)$. This waveobject carries Gaussian distributions over transverse lines that are tilted by angle ϑ with respect to the beam-axis.

space due to sources in $z<0$. We assume that the aperture distribution takes the canonical form of beam-type expansions propagators,

$$u_0(x) = \exp\left[i\omega\left(V_0^{-1} x \cos\vartheta + \frac{1}{2}x^2\Gamma_0 \right)\right], \tag{1}$$

where $V_0=V(0,0)$ with $V(x,z)$ being the medium wave-velocity profile. In Eq. (1) Γ_0 is a frequency-independent complex parameter (the beam's aperture complex curvature) with $\mathrm{Im}\,\Gamma_0>0$, and the spectral angle ϑ is identified as the initial beam-axis angle with respect to the initial x-axis over the $z=0$ plane. Beam field $u(x,z)$ satisfies the 2D inhomogeneous scalar Helmholtz equation

$$[\nabla^2 + \omega^2 V^{-2}(x,z)]u(x,z) = 0, \quad \nabla^2 = \frac{\partial^2}{\partial z^2} + \frac{\partial^2}{\partial x^2}, \tag{2}$$

where $u(x,z)$ is a 2D time-harmonic field with an assumed and suppressed time-dependence of $\exp(-i\omega t)$. Thus we are aiming at obtaining asymptotically exact paraxial solutions to Helmholtz's equation (2) under boundary condition (1) and causality condition of an outgoing wave at $z=0^+$.

3. LOCAL RAY-CENTERED COORDINATE SYSTEM

Following the motivation presented in the introduction, the concept of utilizing non-orthogonal coordinates for beam solutions which was originally introduced in [31,32] is applied here for propagation in generic two-dimensional slowly varying *inhomogeneous media*. We seek beam solutions that are confined about ray trajectories (beam-axes) and apply a local (ray-centered) *non-orthogonal* coordinate system in which the transverse coordinate axis is tilted with respect to the beam-axis and maintains a constant angle of ϑ along the curved trajectory.

The conventional (orthogonal) local ray coordinate system whose origin is located at point $\mathbf{r}_o$ over the ray trajectory is defined by unit-vectors $\hat{\mathbf{t}}_o$ and $\hat{\mathbf{n}}_o$ denoting the tangent and normal of the trajectory at $\mathbf{r}_o$, respectively (see Fig. 2). Here and henceforth, subscript "o" denotes

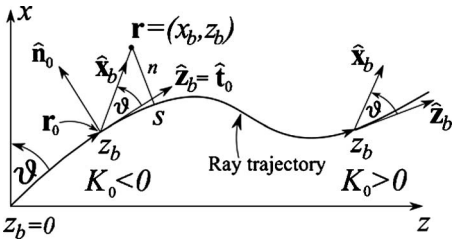

Fig. 2. Observation point $\mathbf{r}$ is described by a non-orthogonal coordinate system $\mathbf{r}=(x_b,z_b)$, where x_b is the distance along the axis that is tilted by ϑ with respect to the ray trajectory tangent, $\hat{\mathbf{t}}_o$, and z_b is the arclength along the trajectory up to the intersection point of the ray with the x_b axis. The (positive) $\hat{\mathbf{x}}_b$ and $\hat{\mathbf{n}}_o$ directions remain constant with respect to the trajectory tangent, and therefore, the curvature $K_o(z_b)$ is negative or positive in convex (left) or concave (right) regions, respectively.

quantities that are sampled at the on-axis coordinate origin $\mathbf{r}_o$. The unit vectors are related by the Fernet equations [33]

$$\frac{d\mathbf{r}_o}{ds} = \hat{\mathbf{t}}_o, \quad \frac{d\hat{\mathbf{t}}_o}{ds} = K_o\hat{\mathbf{n}}_o, \quad \frac{d\hat{\mathbf{n}}_o}{ds} = -K_o\hat{\mathbf{t}}_o, \tag{3}$$

where K_o denotes the curvature of the trajectory at $\mathbf{r}_o$, which for a *ray-trajectory* is given by $K_o=-v_n/v|_{\mathbf{r}_o}$. Here and henceforth, (minuscule) v denotes sampling the velocity profile $V(x,z)$ *on-axis*, v_n denotes the normal on-axis derivative of V, and so forth. We choose a notation in which $\hat{\mathbf{n}}_o$ does not change direction with respect to trajectory tangent, i.e., the unit-vector $\hat{\mathbf{n}}_o\times\hat{\mathbf{t}}_o$ is constant, so that K_o is either negative or positive for convex or concave trajectory intervals, respectively, in accordance with Eqs. (3) (see Fig. 2).

Following the discussion in the introduction, we define a novel *non-orthogonal* coordinate system, in which the local beam coordinate unit-vectors, which are denoted by $\hat{\mathbf{x}}_b$ and $\hat{\mathbf{z}}_b$, are obtained from the conventional (orthogonal) local coordinate unit vectors, $\hat{\mathbf{t}}_o$ and $\hat{\mathbf{n}}_o$, by the transformation

$$\hat{\mathbf{x}}_b = \cos\vartheta\hat{\mathbf{t}}_o + \sin\vartheta\hat{\mathbf{n}}_o, \quad \hat{\mathbf{z}}_b = \hat{\mathbf{t}}_o. \tag{4}$$

Here ϑ is the aperture distribution spectral angle in Eq. (1). The angle ϑ is assumed to be *constant* for all observation points $\mathbf{r}$. Thus, x_b is identified as the distance along an axis that is tilted by ϑ (with respect to the tangent $\hat{\mathbf{t}}_o$), and z_b is the arclength along the trajectory up to the intersection point of the trajectory with the x_b axis (see Fig. 2). Note that the conventional (orthogonal system) tangent parameter s (Eikonal) is a function of both x_b and z_b, namely, $s=s(x_b,z_b)$. Observation point $\mathbf{r}$ can be written in the new coordinates as

$$\mathbf{r} = \mathbf{r}_o(z_b) + x_b\hat{\mathbf{x}}_b, \tag{5}$$

where $\mathbf{r}_o(z_b)$ is the on-axis location of the origin.

In the present context of beam-type (paraxial) solutions, we assume that the on-axis wave-velocity normal deviation away from the beam-axis, $v_n(z_b)$, is small for observation points in the Gaussian domain, i.e., $|v_n(z_b)x_b/v(z_b)|\ll 1$. Thus, we conclude that the trajectory radius of curvature is large with respect to the beam-

width, so that a local (ray-centered) coordinate system can be defined uniquely for all near-axis observation points.

4. MAIN RESULTS

Obtaining beam-type solutions that correspond to the aperture distribution in Eq. (1) involves applying asymptotic approximation of ω-terms rigorously over the ray trajectory. Therefore, for each term in Helmholtz equation (2), a corresponding asymptotic series needs to be obtained in the non-orthogonal ray-centered coordinate system in system (4). This coordinate system is inexplicitly defined along solutions (ray trajectories) of the Eikonal equation. Since this procedure is lengthy, in order to gain clarity in the presentation we first summarize the main results in this section, while full analytic details are given in Section 5.

A. Non-Orthogonal Domain Parabolic Equation

This work presents a new class of paraxial waveobjects of the general ray-field form

$$u(x_b,z_b)=U(\bar{x}_b,z_b)\exp[i\Psi(\bar{x}_b,z_b)], \tag{6}$$

where $U(\bar{x}_b,z_b)$ denotes the ray-field's amplitude,

$$\bar{x}_b=x_b\sqrt{\omega} \tag{7}$$

is the transverse coordinate that is normalized with respect to the frequency ω, and the phase

$$\Psi(\bar{x}_b,z_b)=\omega\int_0^{s(\bar{x}_b,z_b)} v^{-1}(\sigma)d\sigma \tag{8}$$

is accumulated along the ray trajectory arclength σ. Note that unlike the conventional paraxial ray-field, here $U(\bar{x}_b,z_b)$ is described in the local non-orthogonal coordinate system in Eq. (4).

By applying the analytic procedure that is presented below in Subsection 5.B, we find that amplitude U satisfies the novel NoDope in inhomogeneous media,

$$\csc\vartheta v^3(z_b)U_{\bar{x}_b\bar{x}_b}+2i\sin\vartheta v^2(z_b)U_{z_b}-[\bar{x}_b^2\sin^3\vartheta v_{nn}(z_b)+i\sin\vartheta v(z_b)v'(z_b)]U=0, \tag{9}$$

where subscript $\bar{x}_b$, z_b, or n denotes the corresponding partial derivative, such that $U_{z_b}=\partial U/\partial z_b$, etc. By sampling Eq. (4) at $z=0$, we identify $x_b=x$ so that the NoDope in Eq. (9) is solved with the boundary condition

$$U(\bar{x}_b,0)=u(x,0)|_{x=\bar{x}_b/\sqrt{\omega}}\exp[-i\Psi(\bar{x}_b,0)]. \tag{10}$$

Note that by setting $\vartheta=\pi/2$, the NoDope in Eq. (9) reduces to the familiar orthogonal-coordinates parabolic equation in [1,27], and that by setting $V(\mathbf{r})=Const$, we obtain the 2D analog of the homogeneous medium NoDope in [31,32].

B. Tilted GB Solutions

The tilted GBs are localized solutions of NoDope (9) subject to the aperture distributions in Eq. (10). Following the procedure in Subsection 5.C, they are given by

$$U(\bar{x}_b,z_b)=A(z_b)\exp[i\bar{x}_b^2\Gamma(z_b)/2], \tag{11}$$

where the complex curvature

$$\Gamma(z_b)=\sin^2\vartheta p(z_b)/q(z_b) \tag{12}$$

is obtained by solving along the beam-axis the two linear ODEs

$$\frac{d}{dz_b}\begin{bmatrix}q\\p\end{bmatrix}=\begin{bmatrix}0 & v(z_b)\\ -v_{nn}(z_b)/v^2(z_b) & 0\end{bmatrix}\begin{bmatrix}q\\p\end{bmatrix}. \tag{13}$$

These equations are solved with the "initial" ($z=0$) conditions

$$q(0)=1,\quad p(0)=\frac{\Gamma_0}{\sin^2\vartheta}+\frac{V_0'}{V_0^2}\cot^2\vartheta-\frac{2K_0\cot\vartheta}{V_0}, \tag{14}$$

where $K_0=K_o(z_b=0)$. The amplitude $A(z_b)$ in Eq. (11) is given by

$$A(z_b)=\sqrt{\frac{q(0)}{q(z_b)}\frac{v(z_b)}{v(0)}}. \tag{15}$$

The tilted GB waveobjects can be written explicitly by using Eq. (15) in Eq. (11), and inserting into Eq. (6), giving

$$u(x_b,z_b)=\sqrt{\frac{q(0)}{q(z_b)}\frac{v(z_b)}{v(0)}}\exp\left[i\omega\left(\int_0^{s(x_b,z_b)}\frac{d\sigma}{v(\sigma)}+\frac{1}{2}x_b^2\Gamma(z_b)\right)\right]. \tag{16}$$

The tilted GBs in Eq. (16) are a generalization of the two well-known special case solutions: first, for a *homogeneous medium*, by setting $v=\text{const}$, Eq. (13) can be solved explicitly and the tilted GB takes the form [31]

$$u(x_b,z_b)=\sqrt{\frac{\Gamma(z_b)}{\Gamma_0}}\exp\left[i\omega\left(v^{-1}z_b+\frac{1}{2}x_b^2\Gamma(z_b)\right)\right], \tag{17}$$

where $\Gamma(z_b)=(vz_b\csc^2\vartheta+\Gamma_0^{-1})^{-1}$. The second special case of propagation in an inhomogeneous medium with *orthogonal* coordinate system is obtained by setting $\vartheta=\pi/2$, in Eqs. (16) and (13) and in Eq. (4), giving

$$u(s,n)=\sqrt{\frac{q(0)}{q(s)}\frac{v(s)}{v(0)}}\exp\left[i\omega\left(\int_0^s\frac{1}{v(\sigma)}d\sigma+\frac{1}{2}n^2\Gamma(s)\right)\right]. \tag{18}$$

Here $\Gamma(s)=p(s)/q(s)$, where p and q are obtained by setting $\vartheta=\pi/2$ in Eqs. (13) and (14). Solution (18) is the 2D GB in [1].

The tilted GBs in Eq. (16) have a form similar to the conventional (orthogonal-coordinate) GBs in Eq. (18). The main difference is the complex curvature sampling point; for a given observation point (x,z), the complex curvature of a tilted GB is sampled at the corresponding non-orthogonal system origin, i.e., at z_b, whereas an orthogonal GB requires sampling at the orthogonal system origin — s. Therefore, the computational effort in evaluating these solutions is the same, whereas tilted GBs exhibit enhanced accuracy over the conventional ones, which is demonstrated in Section 6.

C. Properties of the Tilted GB

The properties of the tilted GB in Eq. (16) are determined by the complex curvature $\Gamma(z_b)$. The tilted GB exhibits a Gaussian decay over lines of constant z_b that are tilted by angle ϑ with respect to the beam-axis. Its e^{-1} beam-width in x_b coordinates is given by

$$W(z_b) = \sqrt{8}/\sqrt{\omega \operatorname{Im}\Gamma(z_b)}, \tag{19}$$

where $\Gamma(z_b)$ is obtained by solving Eq. (13) along the beam-axis.

The phase-front radius of curvature at an on-axis point z_b that is denoted here by $\rho(z_b)$ is obtained from the real part quadratic phase term in Eq. (16), namely, $\rho(z_b) = 1/\operatorname{Re}\Gamma(z_b)$. This term parameterizes the phase in the tilted transverse coordinate x_b, i.e., over tilted lines of constant z_b (see Fig. 1). In order to relate $\rho(z_b)$ to the radius of curvature in a canonical paraxial ray-field, we sample Eq. (16) over perpendicular lines of constant s. Since over these lines, for different n values both x_b and z_b vary, we approximate [see Eq. (37)] $x = n/\sin\vartheta + O(\omega^{-1})$, as well as

$$\Gamma(z_b) \approx \Gamma(s) - \Gamma'(z_b)\Delta s, \quad \Delta s = s - z_b. \tag{20}$$

Later on in Eq. (37), we establish $\Delta s = O(\omega^{-1/2})$, so that the leading asymptotic term of the real part of the quadratic phase in Eq. (16) reads

$$\operatorname{Re}\left[\frac{1}{2}x_b^2\Gamma(z_b)\right] \approx \frac{1}{2}n^2 \operatorname{Re}[\Gamma(s)]/\sin^2\vartheta. \tag{21}$$

By inserting Eq. (21) into Eq. (16) we can evaluate the phase-front radius of curvature normal to the beam-axis as $\rho_N(z_b) = \sin^2\vartheta/\operatorname{Re}\Gamma(z_b)$. Note that the beam collimation length, which is determined by the complex curvature along the beam-axis, $\Gamma(z_b)$, is frequency independent. Such beam solutions were termed iso-diffracting [34]. The iso-diffracting feature makes these waveobjects highly suitable for time-domain analysis [10,16,17,21,35,36].

5. ANALYTIC DETAILS

Full analytic details of the derivation of the NoDope in Eq. (9) and its tilted GB solutions in Eq. (16) that were presented in Section 4 are given in detail in this section. The procedure introduces a rigorous analysis in terms of asymptotic orders in the ray-centered non-orthogonal coordinate system in Eq. (4).

A. Metric Coefficients

A differential change in $\mathbf{r}$ in Eq. (5) due to infinitesimal displacement along the coordinates curves can be expressed by

$$d\mathbf{r} = \frac{\partial \mathbf{r}}{\partial z_b}dz_b + \frac{\partial \mathbf{r}}{\partial x_b}dx_b. \tag{22}$$

By using Eqs. (5) and (3) in Eq. (22) we obtain the two *unitary-vectors* of this 2D coordinate system [37]

$$\begin{aligned}\mathbf{a}_1 &= \partial\mathbf{r}/\partial z_b = \hat{\mathbf{t}}_o + x_b K_o(\cos\vartheta\hat{\mathbf{n}}_o - \sin\vartheta\hat{\mathbf{t}}_o),\\ \mathbf{a}_2 &= \partial\mathbf{r}/\partial x_b = \sin\vartheta\hat{\mathbf{n}}_o + \cos\vartheta\hat{\mathbf{t}}_o.\end{aligned} \tag{23}$$

As in Eq. (3), subscript o denotes sampling *on-axis* at the origin $\mathbf{r}_o$, i.e., $K_o = K_o(z_b)$, etc. The elements $g_{ij} = \mathbf{a}_i \cdot \mathbf{a}_j$ of the 2×2 metric coefficients tensor $\mathbf{G}$ are given by

$$\mathbf{G}(x_b,z_b) = \begin{bmatrix} 1 - 2x_b\sin\vartheta K_o + x_b^2K_o^2 & \cos\vartheta \\ \cos\vartheta & 1 \end{bmatrix}. \tag{24}$$

The inverse (contravariant) metric-tensor is given by

$$\begin{aligned}\mathbf{G}^{-1}(x_b,z_b) &= \begin{bmatrix} g^{z_bz_b} & g^{z_bx_b} \\ g^{x_bz_b} & g^{x_bx_b} \end{bmatrix}\\ &= \frac{1}{h^2}\begin{bmatrix} 1 & -\cos\vartheta \\ -\cos\vartheta & 1 - 2x_b\sin\vartheta K_o + x_b^2K_o^2 \end{bmatrix},\end{aligned} \tag{25}$$

where

$$h(x_b,z_b) = \sqrt{\det(G)} = \sin\vartheta - x_bK_o(z_b). \tag{26}$$

B. Non-Orthogonal Domain Parabolic Equation

The Laplacian operator in a general 2D non-orthogonal system (x^1,x^2) is given by [37]

$$\nabla^2 = \frac{1}{h}\sum_{i=1}^{2}\sum_{j=1}^{2}\frac{\partial}{\partial x^i}\left[g^{ij}h\frac{\partial u}{\partial x^j}\right], \tag{27}$$

where $g^{ij}(x^1,x^2)$ denotes the (i,j)th element of $\mathbf{G}^{-1}$ matrix that corresponds to system (x^1,x^2), and $h(x^1,x^2)$ is defined in Eq. (26). By inserting Eq. (25) with Eq. (26) into Eq. (27), Helmholtz equation (2) in the local *non-orthogonal* system reads

$$\sum_{k=1}^{6} T_k(x_b,z_b) = 0, \tag{28}$$

where

$$\begin{aligned}T_1(x_b,z_b) &= M_1(x_b,z_b)u_{z_b}(x_b,z_b),\\ T_2(x_b,z_b) &= M_2(x_b,z_b)u_{x_b}(x_b,z_b),\\ T_3(x_b,z_b) &= M_3(x_b,z_b)u_{z_bx_b}(x_b,z_b),\\ T_4(x_b,z_b) &= M_4(x_b,z_b)u_{z_bz_b}(x_b,z_b),\\ T_5(x_b,z_b) &= M_5(x_b,z_b)u_{x_bx_b}(x_b,z_b),\\ T_6(x_b,z_b) &= M_6(x_b,z_b)u(x_b,z_b),\end{aligned} \tag{29}$$

with

$$\begin{aligned}M_1(x_b,z_b) &= (hg^{z_bz_b})_{z_b} + (hg^{x_bz_b})_{x_b},\\ M_2(x_b,z_b) &= (hg^{x_bx_b})_{x_b} + (hg^{z_bx_b})_{z_b},\\ M_3(x_b,z_b) &= h(g^{z_bx_b} + g^{x_bz_b}),\\ M_4(x_b,z_b) &= hg^{z_bz_b},\\ M_5(x_b,z_b) &= hg^{x_bx_b},\end{aligned}$$

$$M_6(x_b,z_b) = h\omega^2 V^{-2}(x_b,z_b), \tag{30}$$

in which the g elements are given in Eq. (25). As in Eq. (9) subscript x_b or z_b denotes the corresponding partial derivative. We aim at obtaining asymptotic (paraxial) solutions of Eq. (28) in x_b coordinates. Following conventional paraxial ray-theory [1,2,27,31], we assume in the following derivation, that the transverse coordinate x_b is of the order of $O(1/\sqrt{\omega})$ [see Eq. (16)]. In the following, we expand Helmholtz's equation into power series of ω. To that extent, we introduce the normalized transverse coordinate in Eq. (7), namely $\bar{x}_b = x_b\sqrt{\omega}$. The asymptotic solution is assumed to have the ray-field form in Eq. (6), where phase $\Psi(\bar{x}_b,z_b)$ in Eq. (8) is accumulated along the beam-axis arclength Eikonal $s(\bar{x}_b,z_b)$ and $U(\bar{x}_b,z_b)$ denotes the ray-field amplitude.

Next we insert ray-field (6) into Helmholtz's equation (28) and collect elements of similar ω-order. The phase Ψ in Eq. (6) is given inexplicitly by integration along the ray trajectory. Thus, partial derivatives of the phase include $s(x_b,z_b)$, its derivatives, as well as $v(s)$ and its derivatives, which are all ω-dependent (via x_b). The paraxial equation procedure requires the use of the *on-axis* wave velocity and its derivatives at point $\mathbf{r}_o$. Therefore, we expand $\Delta s \equiv s - z_b$ in ω series. For a given point over the ray trajectory $\mathbf{r}(s) = \mathbf{r}_o + \Delta\mathbf{r}(\Delta s)$ we approximate (see Fig. 3)

$$\Delta\mathbf{r}(\Delta s) \simeq \left.\frac{d\mathbf{r}}{ds}\right|_{\mathbf{r}_o} \Delta s + \frac{1}{2}\left.\frac{d^2\mathbf{r}}{ds^2}\right|_{\mathbf{r}_o} \Delta s^2. \tag{31}$$

The order of this approximation is justified below [after Eq. (37)]. By using the ray-trajectory differential relations in Eq. (3), we evaluate

$$d^2\mathbf{r}/ds^2|_{\mathbf{r}_o} = d\hat{\mathbf{t}}/ds|_{\mathbf{r}_o} = K_o\hat{\mathbf{n}}_o, \tag{32}$$

and by inserting Eq. (32) into Eq. (31), we obtain

$$\Delta\mathbf{r}(\Delta s) = \Delta s\hat{\mathbf{t}}_o + K_o\Delta s^2\hat{\mathbf{n}}_o/2. \tag{33}$$

Recall that subscript o in the above equations denotes sampling at $\mathbf{r}_o$, i.e., at $\Delta s = 0$. Next by using Eq. (33) we evaluate the unit-vector $\hat{\mathbf{t}}(\Delta s)$ at a trajectory point s near $\mathbf{r}_o$ by (up to $O(\Delta s^2)$)

$$\hat{\mathbf{t}}(\Delta s) = \frac{d\mathbf{r}}{ds} = \frac{d\Delta\mathbf{r}(\Delta s)}{d\Delta s} = \hat{\mathbf{t}}_o + K_o\Delta s\hat{\mathbf{n}}_o. \tag{34}$$

Therefore the normal to $\hat{\mathbf{t}}(\Delta s)$ is given by

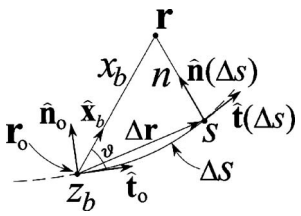

Fig. 3. Δs approximation. The difference between the Eikonal s and the beam local coordinate z_b, $\Delta s = s - z_b$, is expressed in terms of on-axis point $\mathbf{r}_o$ using a Taylor series. Unit-vectors $\hat{\mathbf{n}}_o$ and $\hat{\mathbf{t}}_o$ denote the normal and tangent to the trajectory at $\mathbf{r}_o$, respectively, and unit-vectors $\hat{\mathbf{n}}(\Delta s)$ and $\hat{\mathbf{t}}(\Delta s)$ denote the normal and tangent to the trajectory at point s.

$$\hat{\mathbf{n}}(\Delta s) = \hat{\mathbf{n}}_o - K_o\Delta s\hat{\mathbf{t}}_o. \tag{35}$$

For a given point $\mathbf{r}$ along the x_b axis, we can write $x_b\hat{\mathbf{x}}_b = \Delta\mathbf{r} + n\hat{\mathbf{n}}(\Delta s)$ where n is measured along the normal $\hat{\mathbf{n}}$ from the trajectory to point $\mathbf{r}$. By substituting $\hat{\mathbf{n}}$ in Eq. (35) as well as $\Delta\mathbf{r}$ in Eq. (33), we obtain

$$x_b\hat{\mathbf{x}}_b = \hat{\mathbf{t}}_o\Delta s(1 - K_o n) + \hat{\mathbf{n}}_o(K_o\Delta s^2/2 + n). \tag{36}$$

Finally, by inserting $\hat{\mathbf{x}}_b$ in Eq. (4) to the left-hand-side of Eq. (36) and comparing the two expressions, we obtain the desired approximation for Δs using a Taylor expansion in x_b (recall that $x_b \sim O(\omega^{-1/2})$) as

$$\Delta s = x_b\cos\vartheta(1 + K_o x_b\sin\vartheta) + O(\omega^{-3/2}). \tag{37}$$

Using Eq. (37), we note that x_b and Δs are of the same order of $\omega^{-1/2}$. The following asymptotic formulation requires approximation of Δs up to order ω^{-1} [see Eq. (38)]. Therefore, approximation (31) up to $O(\Delta s^2)$ is justified.

Next we evaluate the asymptotic series of the Eikonal partial derivatives. By using Eq. (37) we approximate (up to ω^{-1})

$$\frac{\partial s}{\partial\bar{x}_b} = \omega^{-1/2}\cos\vartheta + K_o\omega^{-1}\bar{x}_b\sin 2\vartheta + C_{3/2}\omega^{-3/2},$$

$$\frac{\partial s}{\partial z_b} = 1 + \frac{1}{2}K_o'\bar{x}_b^2\omega^{-1}\sin 2\vartheta, \tag{38}$$

where the prime denotes an on-axis derivative with respect to z_b, i.e., $K_o' = dK(z_b)/dz_b|_{\mathbf{r}_o}$. In order to be consistent in the asymptotic procedure, the coefficient $C_{3/2}$ needs to be taken into account. Nevertheless there is no need to evaluate it explicitly, since it cancels out upon insertion into Helmholtz's equation. The on-axis velocity $v(s)$ can now be approximated up to the desired order using a Taylor expansion:

$$v[s(x_b,z_b)] = v_o + \left.\frac{dv}{ds}\right|_{s=z_b}\Delta s + \left.\frac{d^2v}{ds^2}\right|_{s=z_b}\Delta s^2 + O(\Delta s^3). \tag{39}$$

By inserting Δs in Eq. (37), we obtain $v(s) = v_{app}(\bar{x}_b,z_b) + O(\omega^{-3/2})$, in which

$$v_{app}(\bar{x}_b,z_b) = v_o + \omega^{-1/2}\bar{x}_b v_o'\cos\vartheta + \omega^{-1}\bar{x}_b^2[v_o'K_o\sin 2\vartheta + v_o''\cos^2\vartheta]/2. \tag{40}$$

Next we evaluate the partial derivatives in Eq. (30) for ray-field (6). By applying $\partial/\partial z_b$ to Eq. (6) and using Eq. (38), we obtain

$$u_{z_b} = U^{z_b}(\bar{x}_b,z_b)\exp[i\Psi(\bar{x}_b,z_b)], \tag{41}$$

where

$$U^{z_b} = i\omega v^{-1}(z_b)U(\bar{x}_b,z_b) + O(\omega^0). \tag{42}$$

Here and henceforth, we denote U^{z_b} as the amplitude function corresponding to u_{z_b} with respect to the exponent, and so forth. Using this definition, we can evaluate in a similar manner

$$U^{x_b} = \frac{i\omega\cos\vartheta}{v_o}U(\bar{x}_b,z_b) + O(\omega^{1/2}),$$

$$U^{z_bz_b} = -\left[\frac{\omega^2}{v_{app}^2} + \frac{\omega(K_o'\bar{x}_b^2\sin 2\vartheta + iv_o')}{v_o^2}\right]U + \frac{2i\omega}{v(z_b)}U_{z_b} + O(\omega^{1/2}),$$

$$U^{x_bx_b} = -\left[\left(\frac{\partial s}{\partial \bar{x}_b}\right)^2\frac{\omega^3}{v_{app}^2} + \frac{i\omega(v_o'\cos^2\vartheta - K_ov_o\sin 2\vartheta)}{v_o^2}\right]U + \left[\frac{2i\omega K_o\bar{x}_b\sin 2\vartheta}{v_o} + \frac{2i\omega^{3/2}\cos\vartheta}{v_{app}}\right]U_{\bar{x}_b} + \omega U_{\bar{x}_b\bar{x}_b} + O(\omega^{1/2}),$$

$$U^{z_bx_b} = -\left[\frac{\omega^{5/2}}{v_{app}^2}\frac{\partial s}{\partial z_b}\frac{\partial s}{\partial \bar{x}_b} + \frac{i\omega v_o'\cos\vartheta}{v_o^2}\right]U + \frac{i\omega\cos\vartheta}{v_o}U_{z_b} + \left[\frac{i\omega^{3/2}}{v_{app}} - \frac{i\omega v_o'\bar{x}_b\cos\vartheta}{v_o^2}\right]U_{\bar{x}_b} + O(\omega^{1/2}), \quad (43)$$

as well as the M_{1-5} coefficients in Eq. (30):

$$M_1 = -\cot\vartheta\csc\vartheta K_o + O(\omega^{-1/2}),$$

$$M_2 = (\csc^2\vartheta - 2)K_o + O(\omega^{-1/2}),$$

$$M_3 = -2\cot\vartheta(1 + \csc\vartheta K_o\bar{x}_b\omega^{-1/2} + \csc^2\vartheta K_o^2\bar{x}_b^2\omega^{-1}) + O(\omega^{-3/2}),$$

$$M_4 = \csc\vartheta(1 + \csc\vartheta K_o\bar{x}_b\omega^{-1/2} + \csc^2\vartheta K_o^2\bar{x}_b^2\omega^{-1}) + O(\omega^{-3/2}),$$

$$M_5 = \csc\vartheta + (\csc^2\vartheta - 2)K_o\bar{x}_b\omega^{-1/2} + \cot^2\vartheta\csc\vartheta K_o^2\bar{x}_b^2\omega^{-1} + O(\omega^{-3/2}). \quad (44)$$

By inserting ray-field (6) with Eqs. (42)–(44) into Helmholtz's equation (28), we obtain a partial differential equation for amplitude $U(\bar{x}_b,z_b)$.

Next we expand each element in the resulting equation into power series of $\sqrt{\omega}$ up to order of ω [see discussion below following Eq. (50)]. For simplicity, we normalize the T_{1-6} elements in Eq. (28) by the phase exponent $\exp(i\Psi)$, i.e., the normalized T_1, which is denoted by (an overbar) $\bar{T}_1$, is defined as

$$\bar{T}_1 \equiv T_1\exp[-i\Psi] = M_1(\bar{x}_b,z_b)U^{z_b}, \quad (45)$$

and so forth, so that Helmholtz's equation (28) reads

$$\sum_{k=1}^{6}\bar{T}_k(x_b,z_b) = 0. \quad (46)$$

By inserting Eqs. (42) and (44) into Eq. (45) and collecting terms of ω-orders, we obtain

$$\bar{T}_1 = -i\omega\cot\vartheta\csc\vartheta K_ov_o^{-1}U + O(\omega^{1/2}). \quad (47)$$

The same procedure is applied for $\bar{T}_2$–$\bar{T}_5$ terms in Eq. (46), and the resulting expressions are given in Appendix A.

Finally we evaluate the leading ω-components in the last term of the Helmholtz equation (28), namely, $\bar{T}_6$. By expending $V^{-2}(x_b,z_b)$ in Taylor series in the normalized transverse coordinate, $\bar{x}_b$, about the trajectory point $\mathbf{r}_o$, we obtain

$$V^{-2} = \frac{1}{v_o^2} - \omega^{-1/2}\frac{2\bar{x}_b}{v_o^3}v_{x_b} - \omega^{-1}\bar{x}_b^2\left(\frac{v_{x_bx_b}}{v_o^3} - 3\frac{v_{x_b}^2}{v_o^4}\right) + O(\omega^{-3/2}), \quad (48)$$

where (see details in Appendix B)

$$v_{x_b} \equiv \partial V/\partial x_b|_{\mathbf{r}_o} = -\sin\vartheta v_oK_o + \cos\vartheta v_o',$$

$$v_{x_bx_{b_o}} = \sin^2\vartheta v_{nn} + \cos^2\vartheta(v_o'' + K_o^2v_o) - \sin 2\vartheta v_oK_o'. \quad (49)$$

By inserting Eq. (48) with Eqs. (49) and (26) into the last term of Eq. (28) and then expanding into power series of ω, we obtain

$$\bar{T}_6 = v_o^{-3}\left\{\omega^2\sin\vartheta v_o - \omega^{3/2}\bar{x}_b[\cos 2\vartheta K_ov_o + \sin 2\vartheta v_o'] - \omega\bar{x}_b^2\left[\sin^3\vartheta v_{nn} + \sin 3\vartheta K_o^2v_o - \frac{1}{2}(\cos\vartheta + 3\cos 3\vartheta)K_ov_o' - 2\cos\vartheta\sin^2\vartheta K_o'v_o - 3\cos^2\vartheta\sin\vartheta v_o'^2v_o^{-1} + \cos^2\vartheta\sin\vartheta v_o''\right]\right\}U + O(\omega^{1/2}). \quad (50)$$

By inserting series (47), (A.1)–(A.4), as well as Eq. (50), into Helmholtz's equation (46) and collecting coefficients of the same order in ω, we find that the coefficients of ω^2 and $\omega^{3/2}$ cancel out. By setting the highest term, the ω coefficient, to zero we obtain the novel NoDope in inhomogeneous media in Eq. (9).

C. Tilted GB solutions

Following the motivation in the introduction we explore in this subsection solutions of the NoDope in Eq. (9) that are suitable for beam-type expansions. These wave solutions are identified by the aperture distributions in Eq. (1). Thus, we assume that the GBs are of the form in Eq. (11). By inserting $U(z_b,\bar{x}_b)$ in Eq. (11) into the NoDope in Eq. (9), and setting the resulting two coefficients of $\bar{x}_b^2$ and of $\bar{x}_b^0$ to zero, we obtain

$$2\frac{dA}{dz_b}+A(z_b)\left[\csc^2\vartheta v(z_b)\Gamma(z_b)-\frac{v'(z_b)}{v(z_b)}\right]=0, \quad (51)$$

as well as the Ricatti-type equation

$$\Gamma'(z_b)+\csc^2\vartheta v(z_b)\Gamma^2(z_b)+\sin^2\vartheta v^{-2}(z_b)v_{nn}(z_b)=0. \quad (52)$$

The Ricatti equation can be solved by setting

$$\Gamma(z_b)=\sin^2\vartheta q'/(qv), \quad (53)$$

which transforms Eq. (52) into the linear equation

$$v(z_b)q''(z_b)-v'(z_b)q'(z_b)+v_{nn}(z_b)q(z_b)=0. \quad (54)$$

By setting $q'(z_b)=v(z_b)p(z_b)$, we obtain $\Gamma(z_b)$ in Eq. (12), in which p and q are evaluated by solving Eq. (13) along the ray trajectory.

In order to facilitate the "initial" conditions for p and q in Eq. (13), we approximate the aperture distribution in Eqs. (6) and (8) up to the relevant asymptotic orders. First we approximate about the beam's departure point $\sigma=0$:

$$v^{-1}(\sigma)\approx V_0^{-1}-V_0'V_0^{-2}\sigma, \quad (55)$$

where we denote $V_0'=dv(\sigma)/d\sigma|_{\sigma=0}$. By using Eq. (55) we evaluate

$$\int_0^{s(x)}v^{-1}(\sigma)d\sigma\approx\frac{s(x)}{V_0}-\frac{s^2(x)V_0'}{2V_0^2}. \quad (56)$$

The asymptotic terms of $s(x)$ are obtained by substituting $\Delta s=0$, $x_{b_1}=x$, and $z_b=0$ in Eq. (37). By inserting Eqs. (56) and (37) into Eq. (10) with Eq. (11), we obtain the required asymptotic approximation of the tilted GB over $z=0$ plane as

$$u(x,0)=A(0)\exp\left\{i\omega\left[\frac{x\cos\vartheta}{V_0}+\frac{1}{2}x^2\left(\Gamma(0)+\frac{K_0\sin 2\vartheta}{V_0}-\frac{V_0'\cos^2\vartheta}{V_0^2}\right)\right]\right\}. \quad (57)$$

By comparing Eq. (1) with Eq. (57), we identify $A(z_b=0)=1$ and

$$\Gamma(0)=\Gamma_0-K_0V_0^{-1}\sin 2\vartheta+V_0'V_0^{-2}\cos^2\vartheta. \quad (58)$$

Equation (13) is solved along the beam-axis with "initial" conditions $q(0)$ and $p(0)$ such that $\Gamma(0)=\sin^2\vartheta p(0)/q(0)$, for example, the ones presented in Eq. (14).

Finally, the amplitude $A(z_b)$ is found by inserting Eq. (53) into Eq. (51) and evaluating the resulting differential equation by separation of variables. The result is given in Eq. (15). The new GB waveobjects can now be written explicitly by using Eqs. (15) and (12) in Eq. (11), and inserting into Eq. (6). This procedure yields the tilted GB in Eq. (16).

6. NUMERICAL EXAMPLE: PLANE-STRATIFIED MEDIUM

The general solution in Subsection 4.B is applied in this section to z plane-stratified medium with linear velocity profile of

$$V(z)=V_0+\alpha z, \quad z\geqslant 0, \quad (59)$$

where V_0 is the wave-velocity at $z=0$ and α denotes the wave-velocity gradient.

By solving the Eikonal equation for velocity profile (59), one finds that the beam-axis is a circle that is identified by center-point (x_c,z_c) and radius R_0 of

$$(x_c,z_c)=(\tan\vartheta V_0/\alpha,-V_0/\alpha), \quad R_0=V_0/\alpha\cos\vartheta, \quad (60)$$

so that the beam-axis exhibits a turning point at $x_t=x_c$, and

$$z_t=-R_0(1-\sec\vartheta). \quad (61)$$

For a given on-axis point, $\mathbf{r}_0=(x_0,z_0)$,

$$x_0=x_c\mp[R_0^2-(z_0-z_c)^2]^{1/2}, \quad (62)$$

where (x_c,z_c) are given in Eq. (60) and $\mp$ corresponds to observation points before or after the turning point, respectively. The arclength σ along the beam-axis can be easily obtained from Eq. (60), giving

$$\sigma=R_0[\sin^{-1}(\cos\vartheta+z_0/R_0)+\vartheta-\pi/2]. \quad (63)$$

A. Tilted GB Evaluation

Let $\mathbf{r}_{n_0}=(x_{n_0},z_{n_0})$ be the origin of the conventional orthogonal local beam coordinate system (s,n) over ray trajectory (60). For a given observation point $\mathbf{r}=(x,z)$

$$x_{n_0}=R_0\left(\frac{x-x_c}{d}+\sin\vartheta\right), \quad z_{n_0}=R_0\left(\frac{z-z_c}{d}-\cos\vartheta\right), \quad (64)$$

where

$$d(x,z)=\sqrt{(x-x_c)^2+(z-z_c)^2}. \quad (65)$$

By inserting z_{n_0} in Eqs. (64) into Eq. (63), we obtain

$$n=R_0-d, \quad s=R_0\left[\sin^{-1}\left(\frac{x-x_c}{d}\right)+\vartheta\right]. \quad (66)$$

Applying Snell's law to the plane-stratified medium, and using Eq. (63), we observe that the *on-axis* wave-velocity is related to the arclength along the ray via

$$v(\sigma)=V_0\cos(\vartheta-\alpha\sigma\cos\vartheta/V_0)/\cos\vartheta, \quad (67)$$

so that Eq. (13) with initial condition (14) can be solved for medium profile (59) explicitly. Thus, using Eq. (12), $\Gamma(\sigma)=\sin^2\vartheta p(\sigma)/q(\sigma)$ where

$$p(\sigma) = p(0),$$

$$q(\sigma) = 1 + \frac{V_0^2}{\alpha}\frac{p(0)}{\cos^2\vartheta}\left[\sin\left(\vartheta - \cos\vartheta\frac{\alpha\sigma}{V_0}\right) - \sin\vartheta\right], \tag{68}$$

where $p(0)$ is given in Eq. (14). For observation point $\mathbf{r}=(x,z)$, the (x_b,z_b) coordinates in the local *non-orthogonal* system, are obtained by using basic trigonometry:

$$x_b = \pm R_o[\sqrt{(1-n/R_o)^2 - \cos^2\vartheta} - \sin\vartheta], \quad d \gtrless R_o,$$

$$z_b = s - R_o \sin^{-1}[x_b\cos\vartheta/(R_o - n)]. \tag{69}$$

Thus, the (x_b,z_b) coordinates in terms of (x,z) coordinates are obtained by inserting $d(x,y)$ in Eq. (65) with Eq. (60) into Eqs. (69), and the analytic tilted GB at point (x,z) is obtained by inserting the resulting (x_b,z_b) into Eq. (16) with σ in Eq. (63), $v(\sigma)$ in Eq. (67), and $p(\sigma)$ and $q(\sigma)$ in Eqs. (68).

B. Conventional GB Evaluation

The conventional GB solution in Eq. (18) is obtained by projecting the aperture complex curvature, Γ_0, on a plane normal to the beam initial direction. Thus the conventional aperture complex curvature is $\Gamma_{N_0}(0)=\Gamma_0/\sin^2\vartheta$, and the conventional beam field is obtained by solving Eq. (13) along the ray trajectory, with initial condition Γ_{N_0} [that is, by replacing Γ_0 with Γ_{N_0} in Eq. (18)]. Coordinates (n,s) are given in Eqs. (66), and p and q are given in Eqs. (68) with $\sigma=s$ and $p(0)=\Gamma_{N_0}$.

C. Reference Field Evaluation

The reference field is obtained by applying the Fourier transform in the x direction and propagating the resulting *local* plane-wave spectra via the WKBJ approximation. Thus the reference field in $z>0$, which is denoted here by $u_{ref}(x,z)$, is given by the following spectral representation [38,39]:

$$u_{ref}(x,z) = \frac{1}{V_0}\sqrt{\frac{i\omega}{2\pi\Gamma_0}}\int d\xi C(\xi) \times\left(\frac{1-\xi^2}{\zeta^2(z,\xi)}\right)^{1/4}\exp[i\omega\tilde{\Psi}(x,z;\xi)],$$

$$\tilde{\Psi}(x,z;\xi) = \left[\frac{(\cos\vartheta - \xi)^2}{2V_0^2\Gamma_0} + V_0^{-1}\int_0^z \zeta(z',\xi)dz' + V_0^{-1}\xi x\right], \tag{70}$$

where $\zeta(z,\xi)=\sqrt{V_0^2/V^2(z)-\xi^2}$, $\mathrm{Im}\,\zeta\geqslant 0$, and $C(\xi)$ is given by

$$C(\xi) = 1 - i\exp\left\{\frac{2i\omega}{V_0}\left[\int_0^{z_t(\xi)}\zeta(z',\xi)dz' - \int_0^z \zeta(z',\xi)dz'\right]\right\}. \tag{71}$$

In Eqs. (70) and (71), $z_t(\xi)$ denotes the turning point of a local plane-wave with spectral variable ξ where $\zeta(z_t,\xi)=0$. The second term in Eq. (71) is identified as the caustic reflection coefficient of the local plane-wave of spectral ξ. By applying the saddle-point procedure to the phase integral in Eqs. (70) one can easily observe that the local plane-waves in the spectral representation interfere constructively along and in the vicinity of the beam-axis that emanates from the origin with angle ϑ with respect to the x-axis.

The $[-\infty,\infty]$ integration in Eqs. (70) is numerically implemented by integration over an effective contribution interval around the phase on-axis stationary point, $\xi_s=\xi_0=\cos\vartheta$, i.e., $[\xi_0-\Delta\xi,\xi_0+\Delta\xi]$. We set the spectral interval $\Delta\xi=\sqrt{Mc^2/\mathrm{Im}\{\Gamma_0^{-1}\}\omega}$, which corresponds to the maximal spectrum attenuation of e^{-M}. The sampling rate $\delta\xi$ is chosen according to $\delta\xi\ll\Delta\xi/M$, so that the sampling rate is small on the scale of the integrand oscillation period. It was found that in order to achieve a numerical convergence with a maximal relative error of 10^{-5} on-axis it is sufficient to choose $M=5$ and $\delta\xi=10^{-3}\Delta\xi/M$.

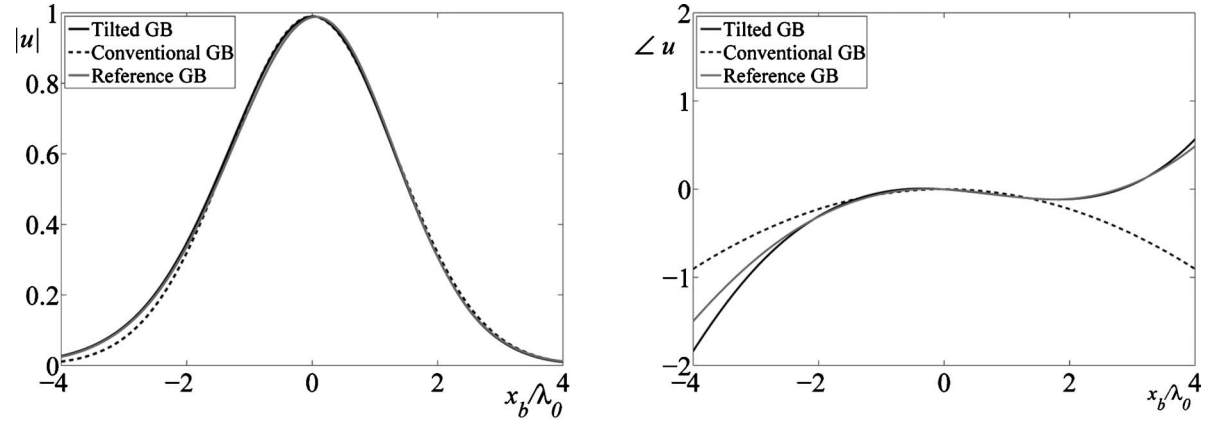

(a) (b)

Fig. 4. Tilted GB (solid curve), the conventional GB (dashed curve), and the reference field (light gray) curves that are sampled over a line perpendicular to the beam-axis. (a) Absolute value, (b) phase in radians. The inhomogeneous parameters are $V_0=1$, $\alpha=0.01$, and the fields parameters are $\omega=5000$, $\Gamma_0=i/3$, $\vartheta=15^o$, and $s_m=32\lambda_0$.

D. Error Comparison

In Fig. 4 we plot the tilted GB (solid curve), the conventional GB (dashed curve) and the reference field (light gray) curves that are sampled over a line perpendicular to the beam-axis (where the conventional GB carries a symmetrical Gaussian distribution). The line intersects the beam-axis at arclength $s_m=32\lambda_0$, where $\lambda_0=2\pi V_0/\omega$ denotes the local wavelength at the beam's departure point. The inhomogeneous medium is given in Eq. (59) with $V_0=1$, $\alpha=0.01$, and the field parameters are $\omega=5000$, $\Gamma_0=i/3$, and $\vartheta=15^o$. Figures 4(a) and 4(b) presents the field's absolute value and phase (in radians), respectively, as a function of x_b/λ_0. The plots reveal good agreement between the tilted GB and the reference field, whereas the conventional GB plots exhibit a significant error in the off-axis field, especially in the phase (Fig. 4(b)), where the reference and tilted GBs are not symmetrical with respect to the $x_b=0$ on-axis point.

In Fig. 5 we compare the tilted GB $\mathbb{L}_2$ error norm with respect to the reference field (70) to the corresponding error of the conventional GB. The error is evaluated along an observation line that is normal to the beam-axis and is located at an on-axis arclength of s_m, according to the norm definition

$$\mathbb{L}_2[u,u_{ref}]=\sqrt{\frac{1}{L}\int_{-L/2}^{L/2}|u(s_m,n)-u_{ref}(s_m,n)|^2dn}, \quad (72)$$

where u denotes either the tilted or the conventional GB and n denotes the conventional (orthogonal system) normal coordinate.

The figure plots the relative error with respect to the on-axis reference field, $u_{ref}(s_m,0)$, in percent as a function of the on-axis location s_m, which is normalized by the *homogeneous* medium collimation length $F_h=V_0\sin^2\vartheta\,\mathrm{Im}\,\Gamma_0^{-1}$ [31]. The error was evaluated for three different ϑ values: 10°, 20°, and 30°. Here we set $\mathrm{Re}\,\Gamma_0=0$ so that the waists are located on the $z=0$ plane. The curves are arranged in pairs with continuous and dashed lines, corresponding to errors of the tilted GB and the conventional one, respectively. Each of the curve pairs in Fig. 5 share a common gray shade corresponding to the field's spectral angle ϑ.

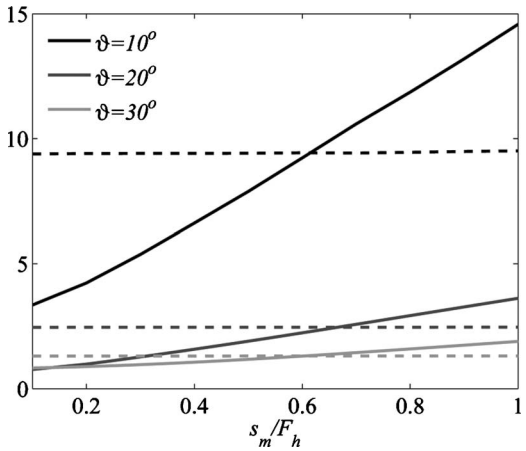

Fig. 5. $\mathbb{L}_2$ error norms of the tilted and approximated GBs in percent as a function of the normalized on-axis arclength s_m/F_h are plotted for three different values of ϑ. The curves are arranged in pairs with continuous and dashed lines corresponding to errors of the tilted GB and the approximated one, respectively. The medium and field parameters are as in Fig. 4. The figure demonstrates the enhanced accuracy of tilted GBs within the collimated beam domain $s_m<0.7F_h$.

The figure demonstrates that for $s_m/F_h<0.7$ tilted GBs exhibit better accuracy over the conventional beams, that is in the *well-collimated* regime. Note that beam-type expansions are used so as to take advantage of the analytic simplicity that is introduced by the spatial and spectral localization of these waveobjects. Thus, these expansion schemes are tuned such that the GBs remains *well-collimated* within all domains of interest. Similar results were obtained for homogeneous media in [32].

7. CONCLUDING REMARKS

We have presented the concept of utilizing non-orthogonal coordinates for tilted GB propagation in 2D inhomogeneous media, in order to obtain asymptotically exact beam type solutions to the wave equation in the time-harmonic regime. By utilizing these novel coordinates, we attained in Eq. (9) a novel non-orthogonal generalization of the paraxial wave equation which was termed NoDope. While the procedure of obtaining the NoDope in a homogeneous medium [31] is straightforward, the corresponding procedure in inhomogeneous media exhibits an additional degree of complexity due to the inexplicit expressions for the ray-field form in which the phase is given by integration along ray trajectories. Applying a consistent asymptotic procedure in ray centered non-orthogonal coordinates was feasible, and a generic novel parabolic wave equation was obtained.

Asymptotically exact beam-type solutions to the NoDope were presented and termed *tilted Gaussian beams*. Comparing the tilted GB fields to the conventional (orthogonal) ones, it was found that the two have essentially the same form. The difference is in the complex curvature Γ sampling point and in transverse coordinate $\mathbf{x}_b$ values. For a given observation point, $\mathbf{r}$, the complex curvature in the tilted GB solution is sampled on-axis at the origin of the non-orthogonal coordinate system z_b, whereas in the conventional solution it is sampled on-axis at the origin of the orthogonal system.

The present work introduced a new family of asymptotic beam-solutions *a priori* matched to Gaussian distributions over planes that are tilted with respect to the beam-axes. Through numerical example we demonstrated that tilted GBs exhibit enhanced accuracy over the conventional ones in the well-collimated regime. Thus, these novel waveobjects whose numerical evaluation is as cost effective as the conventional ones can be considered as another significant contribution to beam-type spectral expansion schemes.

APPENDIX A: EXPLICIT EXPRESSIONS FOR $\bar{T}_{2-5}$

Following the procedure that was introduced in Eqs. (45) and (47), we obtain for $\bar{T}_j$, $j=2-5$:

$$\bar{T}_2=i\omega\frac{\cot\vartheta\cos 2\vartheta\csc\vartheta K}{v_o}U+O(\omega^{1/2}), \quad (A.1)$$

$$\bar{T}_3 = \left\{ \omega^2 \frac{2\cos\vartheta\cot\vartheta}{v_o^2} + \omega^{3/2}\bar{x}_b \cot\vartheta\left(\frac{2(\cot\vartheta + \sin 2\vartheta)K}{v_o^2} - \frac{4\cos^2\vartheta v_o'}{v_o^3} \right) + \omega\left[6\bar{x}_b^2 \frac{\cos^3\vartheta\cot\vartheta v_o'^2}{v_o^4} + 2C_{3/2}\frac{\cot\vartheta}{v_o^2} \right.\right.$$
$$+ 2\bar{x}_b^2 \frac{(2\cos\vartheta\cot\vartheta + \cot^2\vartheta\csc\vartheta)K^2}{v_o^2} + 2\bar{x}_b^2\frac{\cos^3\vartheta K'}{v_o^2} + 2i\frac{\cot\vartheta\cos\vartheta v_o'}{v_o^2} - 2\bar{x}_b^2\cos\vartheta\cot\vartheta\left(\frac{(5-3\cos 2\vartheta)\cot\vartheta K v_o'}{v_o^3} \right.$$
$$\left.\left.\left. + \frac{\cos^2\vartheta v_o''}{v_o^3} \right) \right] \right\} U - \left[i\omega^{3/2}\frac{2\cot\vartheta}{v_o} + i\omega\bar{x}_b\left(\frac{2\cot\vartheta\csc\vartheta K}{v_o} - \frac{2\cos\vartheta\cot\vartheta v_o'}{v_o^2} \right) \right] U_{\bar{x}_b} - i\omega\frac{2\cot\vartheta\cos\vartheta}{v_o} U_{z_b} + O(\omega^{1/2}), \tag{A.2}$$

$$\bar{T}_4 = \left[-\omega^2\frac{\csc\vartheta}{v_o^2} + \omega^{3/2}\bar{x}_b\left(\frac{2\cot\vartheta v_o'}{v_o^3} - \frac{\csc^2\vartheta K}{v_o^2} \right) - \omega\csc\vartheta\left(\bar{x}_b^2\frac{\csc^2\vartheta K^2}{v_o^2} + \frac{1}{2}\bar{x}_b^2\frac{(\cos 3\vartheta - 5\cos\vartheta)\csc\vartheta K v_o'}{v_o^3} + \frac{\bar{x}_b^2\sin 2\vartheta K' + i v_o'}{v_o^2} \right.\right.$$
$$\left.\left. + 3\bar{x}_b^2\frac{\cos^2\vartheta v_o'^2}{v_o^4} - \bar{x}_b^2\frac{\cos^2\vartheta v_o''}{v_o^3} \right) \right] U + i\omega\frac{2\csc\vartheta}{v_o} U_{z_b} + O(\omega^{1/2}), \tag{A.3}$$

$$\bar{T}_5 = \left[-\omega^2\frac{\cos\vartheta\cot\vartheta}{v_o^2} + \omega^{3/2}\bar{x}_b\frac{\cot\vartheta\csc\vartheta}{2}\left(\frac{(\cos 3\vartheta - 3\cos\vartheta)K}{v_o^2} + 4\frac{\sin\vartheta\cos^2\vartheta v_o'}{v_o^3} \right) + \omega\left(2i\frac{\cos\vartheta K}{v_o} - 3\bar{x}_b^2\frac{\cos^3\vartheta\cot\vartheta v_o'^2}{v_o^4} \right.\right.$$
$$- 2C_{3/2}\frac{\cot\vartheta}{v_o^2} + \bar{x}_b^2\frac{\cos\vartheta\cot^3\vartheta(2\cos 2\vartheta - 3)K^2}{v_o^2} - i\frac{\cos\vartheta\cot\vartheta v_o'}{v_o^2} + \bar{x}_b^2\cos\vartheta\cot\vartheta\left(\frac{(5-3\cos 2\vartheta)\cot\vartheta K v_o'}{v_o^3} + \frac{\cos^2\vartheta v_o''}{v_o^3} \right)\left.\left.\right) \right] U$$
$$+ \left[i\omega^{3/2}\frac{2\cot\vartheta}{v_o} + i\omega\bar{x}_b\left(\frac{2\cot\vartheta\csc\vartheta K}{v_o} - \frac{2\cos\vartheta\cot\vartheta v_o'}{v_o^2} \right) \right] U_{\bar{x}_b} + \omega\csc\vartheta U_{\bar{x}_b\bar{x}_b} + O(\omega^{1/2}). \tag{A.4}$$

APPENDIX B: DERIVATION OF EQUATION (49)

The gradient operator in terms of the *orthogonal* ray-centered coordinates (s,n) is given by

$$\nabla = \hat{\mathbf{n}}\partial_n + \hat{\mathbf{t}}h^{-1}\partial_s, \tag{B.1}$$

with

$$h = 1 - K(s)n, \tag{B.2}$$

where $(1,h)$ are the orthogonal coordinate metric coefficients. The derivative in the direction of the unit-vector $\hat{\mathbf{x}}_b$ is given by

$$\partial_{x_b} = (\hat{\mathbf{x}}_b\cdot\hat{\mathbf{n}})\partial_n + h^{-1}(\hat{\mathbf{x}}_b\cdot\hat{\mathbf{t}})\partial_s. \tag{B.3}$$

In order to evaluate ∂_{x_b} on-axis, we set $x_b=0$ (or $n=0$), $h=1$, $\hat{\mathbf{t}}=\hat{\mathbf{t}}_o$, $\hat{\mathbf{n}}=\hat{\mathbf{n}}_o$, $s=z_b$ and $\partial_s=\partial_{z_b}$ in Eq. (B.3). Thus, on-axis

$$\partial_{x_b} = \sin\vartheta\partial_n + \cos\vartheta\partial_{z_b}. \tag{B.4}$$

The second directional derivative in the direction of $\hat{\mathbf{x}}_b$ is given by

$$\partial_{x_b x_b} = \hat{\mathbf{x}}_b\cdot\nabla(\hat{\mathbf{x}}_b\cdot\nabla) = [(\hat{\mathbf{x}}_b\cdot\hat{\mathbf{n}})\partial_n\nabla\cdot\hat{\mathbf{x}}_b + h^{-1}(\hat{\mathbf{x}}_b\cdot\hat{\mathbf{t}})\partial_s\nabla\cdot\hat{\mathbf{x}}_b]. \tag{B.5}$$

Since unit-vectors $(\hat{\mathbf{t}},\hat{\mathbf{n}})$ are invariant with respect to normal coordinate n, by applying either ∂_n or ∂_s to Eq. (B.1) and inserting Eq. (3), we obtain, respectively,

$$\partial_n\nabla = \hat{\mathbf{n}}\partial_{nn}^2 + \hat{\mathbf{t}}[h^{-1}\partial_{sn}^2 + K(s)h^{-2}\partial_s], \tag{B.6}$$

and

$$\partial_s\nabla = \hat{\mathbf{n}}[\partial_{sn}^2 + K(s)h^{-1}\partial_s] + \hat{\mathbf{t}}[h^{-1}\partial_{ss}^2 - h_s h^{-2}\partial_s - K(s)\partial_n]. \tag{B.7}$$

By inserting Eqs. (B.6), (B.7), and (3) into Eq. (B.5) and sampling on-axis at $\mathbf{r}_o$, we obtain

$$\partial_{x_b x_b} = \cos^2\vartheta\partial_{z_b}^2 + \sin 2\vartheta\partial_{nz_b}^2 + \sin^2\vartheta\partial_{nn}^2 + \sin 2\vartheta K_o\partial_{z_b} - \cos^2\vartheta K_o\partial_n. \tag{B.8}$$

Finally, using $K_o=-v_n(z_b)/v(z_b)$ in Eq. (B.8), we obtain the final result in Eq. (49).

REFERENCES

1. V. Cerveny, M. M. Popov, and I. Pŝencik, "Computation of wave fields in inhomogeneous media—Gaussian beam approach," Geophys. J. R. Astron. Soc. **70**, 109–128 (1982).
2. E. Heyman, "Pulsed beam propagation in an inhomogeneous medium," IEEE Trans. Antennas Propag. **42**, 311–319 (1994).
3. T. Melamed, "Phase-space Green's functions for modeling time-harmonic scattering from smooth inhomogeneous objects," J. Math. Phys. **46**, 2232–2246 (2004).
4. S. Y. Shin and L. B. Felsen, "Gaussian beams in anisotropic media," Appl. Phys. **5**, 239–250 (1974).
5. R. Simon and N. Mukunda, "Shape-invariant anisotropic Gaussian Schell-model beams: a complete characterization," J. Opt. Soc. Am. A **15**, 1361–70 (1998).

6. E. Poli, G. V. Pereverzev, and A. G. Peeters, "Paraxial Gaussian wave beam propagation in an anisotropic inhomogeneous plasma," Phys. Plasmas **6**, 5–11 (1999).
7. L. I. Perez and M. T. Garea, "Propagation of 2D and 3D Gaussian beams in an anisotropic uniaxial medium: vectorial and scalar treatment," Optik **111**, 297–306 (2000).
8. I. Tinkelman and T. Melamed, "Gaussian beam propagation in generic anisotropic wavenumber profiles," Opt. Lett. **28**, 1081–1083 (2003).
9. I. Tinkelman and T. Melamed, "Local spectrum analysis of field propagation in anisotropic media. I. Time-harmonic fields," J. Opt. Soc. Am. A **22**, 1200–1207 (2005).
10. I. Tinkelman and T. Melamed, "Local spectrum analysis of field propagation in anisotropic media. II. Time-dependent fields," J. Opt. Soc. Am. A **22**, 1208–1215 (2005).
11. A. G. Khatkevich, "Propagation of pulses and wave packets in dispersive gyrotropic crystals," J. Appl. Spectrosc. **46**, 203–207 (1987).
12. T. Melamed and L. B. Felsen, "Pulsed beam propagation in lossless dispersive media. I. Theory," J. Opt. Soc. Am. A **15**, 1268–1276 (1998).
13. T. Melamed and L. B. Felsen, "Pulsed beam propagation in lossless dispersive media. II. A numerical example," J. Opt. Soc. Am. A **15**, 1277–1284 (1998).
14. T. Melamed and L. B. Felsen, "Pulsed beam propagation in dispersive media via pulsed plane wave spectral decomposition," IEEE Trans. Antennas Propag. **48**, 901–908 (2000).
15. A. P. Kiselev, "Localized light waves: paraxial and exact solutions of the wave equation (a review)," Opt. Spectrosc. **102**, 603–622 (2007).
16. A. Shlivinski, E. Heyman, A. Boag, and C. Letrou, "A phase-space beam summation formulation for ultra wideband radiation," IEEE Trans. Antennas Propag. **52**, 2042–2056 (2004).
17. A. Shlivinski, E. Heyman, and A. Boag, "A pulsed beam summation formulation for short pulse radiation based on windowed radon transform (WRT) frames," IEEE Trans. Antennas Propag. **53**, 3030–3048 (2005).
18. T. Melamed, "Exact beam decomposition of time-harmonic electromagnetic waves," J. Electromagn. Waves Appl. **23**, 975–986 (2009).
19. B. Z. Steinberg, E. Heyman, and L. B. Felsen, "Phase space beam summation for time-harmonic radiation from large apertures," J. Opt. Soc. Am. A **8**, 41–59 (1991).
20. B. Z. Steinberg, E. Heyman, and L. B. Felsen, "Phase space beam summation for time dependent radiation from large apertures: Continuous parametrization," J. Opt. Soc. Am. A **8**, 943–958 (1991).
21. T. Melamed, "Phase-space beam summation: A local spectrum analysis for time-dependent radiation," J. Electromagn. Waves Appl. **11**, 739–773 (1997).
22. M. A. Leontovich and V. A. Fock, "Solution of the problem of EM wave propagation along the earth surface by the parabolic equation method," J. Phys. **10**, 13 (1946).
23. G. D. Malyuzhinets, "Progress in understanding diffraction phenomena (in Russian)," Sov. Phys. Usp. **69**, 321–334 (1959).
24. A. V. Popov, "Numerical solution of the wedge diffraction problem by the transversal diffusion method (in Russian)," Sov. Phys. Acoust. **15**, 226–233 (1969).
25. S. N. Vlasov and V. I. Talanov, "The parabolic equation in the theory of wave propagation," Radiophys. Quantum Electron. **38**, 1–12 (1995).
26. M. Levys, *Parabolic Equation Methods for Electromagnetic Wave Propagation* (The Institution of Electrical Engineers, 2000).
27. C. Chapman, *Fundamentals of Seismic Wave Propagation* (Cambridge Univ. Press, 2004).
28. J. A. Arnaud and H. Kogelnik, "Gaussian light beams with general astigmatism," Appl. Opt. **8**, 1687–1693 (1969).
29. G. A. Deschamps, "Gaussian beam as a bundle of complex rays," Electron. Lett. **7**, 684–685 (1971).
30. S. D. Patil, S. T. Navare, M. V. Takale, and M. B. Dongare, "Self-focusing of cosh-Gaussian laser beams in a parabolic medium with linear absorption," Opt. Lasers Eng. **47**, 604–606 (2009).
31. Y. Hadad and T. Melamed, "Non-orthogonal domain parabolic equation and its Gaussian beam solutions," IEEE Trans. Antennas Propag. **58**, 1164–1172 (2010).
32. Y. Hadad and T. Melamed, "Parameterization of the tilted Gaussian beam waveobjects," PIER **102**, 65–80 (2010).
33. V. M. Babič and V. S. Buldyrev, *Short-Wavelength Diffraction Theory: Asymptotic Methods* (Springer-Verlag, 1991).
34. E. Heyman and T. Melamed, "Certain considerations in aperture synthesis of ultrawideband/short-pulse radiation," IEEE Trans. Antennas Propag. **42**, 518–525 (1994).
35. E. Heyman and T. Melamed, "Space-time representation of ultra wideband signals," in *Advances in Imaging and Electron Physics*, Vol. 103 (Elsevier, 1998), pp.1–63.
36. A. Shlivinski, E. Heyman, and A. Boag, "A phase-space beam summation formulation for ultrawide-band radiation—Part II: A multiband scheme," IEEE Trans. Antennas Propag. **53**, 948–957 (2005).
37. A. P. Wills, *Vector Analysis with an Introduction to Tensor Analysis* (Dover, 1958).
38. W. C. Chew, *Waves and Fields in Inhomogeneous Media* (IEEE, 1995).
39. E. Heyman and L. B. Felsen, "Real and complex spectra—a generalization of WKBJ seismograms," Geophys. J. R. Astron. Soc. **91**, 1087–1126 (1987).